A MULTISCALE DAMAGE ANALYSIS OF PERIODIC COMPOSITES USING A COUPLE-STRESS/CAUCHY MULTIDOMAIN MODEL: APPLICATION TO MASONRY STRUCTURES

Lorenzo Leonetti[1]**, Fabrizio Greco**[2]**, Patrizia Trovalusci**[1]**, Raimondo Luciano**[3], **Renato Masiani**[1]

[1] Department of Structural and Geotechnical Engineering, Sapienza University of Rome, Italy
Via A. Gramsci, 53, 00197, Rome, Italy
e-mail: {lorenzo.leonetti, patrizia.trovalusci, renato.masiani}@uniroma1.it

[2] Department of Civil Engineering, University of Calabria, Italy
Via P. Bucci, Cubo 39B, 87036, Rende, Italy
e-mail: f.greco@unical.it

[3] Department of Civil and Mechanical Engineering, University of Cassino and Southern Lazio, Italy
Via Di Biasio, 43, 03043, Cassino, Italy
e-mail: luciano@unicas.it

Keywords: Couple-Stress Continua, Multiscale Methods, Masonry, Homogenization, Damage, Composite Structures.

Abstract. *A novel multiscale strategy is proposed for the damage analysis of masonry structures modeled as periodic composites. Such a computational strategy, whose aim is to reduce the typically high computational cost exhibited by fully microscopic numerical analyses, is based on a multiscale/multidomain model equipped with an adaptive capability, which allows to automatically zoom-in the zones incipiently affected by damage onset. The associated model refinement criterion requires the determination of microscopically informed first failure surfaces, which take into account both classical and bending deformation effects, by taking advantage of a couple-stress based homogenization technique. In order to assess the efficacy of the proposed multiscale modeling strategy, some numerical simulations are presented, involving a medium-sized wall test subjected to combined shear and flexure loading conditions. The related accuracy and computational performances of this methodology are investigated via suitable comparisons with a purely discrete model of masonry. Special attention is devoted to the analysis of the bending macroscopic deformation effects. Further comparisons with experimental results taken from the literature are carried out in order to validate its predictive capability in terms of peak and post-peak mechanical behavior.*

1 INTRODUCTION

At a conventionally defined microscopic scale, masonry can be regarded as a particle composite material, made of at least two components, i.e. the units (bricks, stones, blocks) and the mortar joints. This modeling is more indicated when studying modern masonry, but can be applied also to historic masonry, in which the units are separated by dry joints. In the latter case, the joints turn to be simply considered as cohesionless interfaces and the whole masonry may be modeled as an ensemble of rigid block interacting to each other according to contact with friction interactions.

At this scale of observation, the most natural modeling strategy consist in using *discrete models* for the entire masonry structure, to be used for direct numerical simulations, able to take into account all the underlying microstructural details [1–4]. Obviously, this type of modeling requires an enormous amount of computational resources, especially when damage-induced nonlinearities are included in the constitutive behavior of masonry components.

On the other hand, *continuous models* are suitable for investigating the overall behavior of large masonry structures, due to their intrinsic computational efficiency. Continuous modeling has been successfully employed in many practical applications of civil engineering, and specifically for studying the behavior of real-life unreinforced masonry structures under seismic actions [5–7]. As a matter of fact, this type of analysis is mandatory when dealing with the design of retrofitting and strengthening interventions, as those based on the use of externally applied FRP or FRCM reinforcement systems [8–16].

In fact, these models don't distinguish any masonry component, but consider masonry material as a whole at a conventionally defined macroscopic scale. To this end, a macroscopic constitutive behavior of masonry should be properly identified. The first approaches pursed in the technical literature to characterize the masonry material were of a phenomenological type [17–19]. These approaches often are difficult to handle, due to the high number of properties to be experimentally derived. This is related to the complexity of masonry response even in the linear range, due to its intrinsic anisotropic nature.

As an alternative to phenomenological models, homogenized models have been extensively used to derive macroscopic models for masonry, where equivalent coarse-scale homogenized elements are used in place of the original combination of brick and mortar materials. These approaches have been shown to be very effective for modeling masonry in the linear range [20–24], but some difficulties have been experienced when the final aim is to capture the inherent nonlinear composite behavior.

A more general framework for obtaining the overall response of heterogeneous materials (including masonry-like ones) taking into account the influence of all the microscopic nonlinearities is the so-called multiscale modeling, which combine the advantages of purely macroscopic (i.e. computational efficiency) and microscopic models (i.e. numerical accuracy) [25].

In the last decades, several multiscale methods have been used to predict the mechanical response of heterogeneous materials in both linear and nonlinear ranges, with a special attention to fiber- and particle-reinforced composites, polycrystals and concrete-like materials (see [26–33]). These methods have been applied also to simulate the damage phenomena in masonry structures under complex loading conditions, mainly based on the definition of the failure surfaces obtained through micro-mechanical homogenization approaches [34–41]. In this context, the most common strategy consists in deriving the overall nonlinear response via computational homogenization methods (also called global-local approaches) based on the concept of scale transition, by which the information is passed from lower to higher scales and vice versa (see, for instance, [37]). However, such a strategy is very effective in the presence of moderate localization, but necessary fails when the size of localization band results to be smaller than the dimensions of the representative volume element (RVE) or repeating cell (RC).

As an alternative to the well-established computational homogenization methods, different versions of concurrent multiscale methods have been applied for the first time to the damage analysis of masonry structures in previous works by some of the authors [42,43]. These methods, relying on the concept of scale embedding, can be considered as a multilevel version of well-known domain decomposition methods. In fact, the original spatial domain is decomposed into two sets of non-overlapping subdomains, the first being modeled at the macroscopic scale (with overall properties obtained via a first-order homogenization in the linear range) and the second described at a conventionally defined microscopic scale, responsible for taking into account the nonlinear effects due to microscopic damage evolution. As the location of damage initiation and evolution is not known a priori in general, these multiscale methods are equipped with an adaptive capability, meaning that the model is able to automatically refine itself according a suitable defined zooming-in criterion based on the first failure detection at the microscopic scale.

Encouraged by the results obtained using these methods, we propose an enhanced multiscale model for the nonlinear analysis of periodic masonries under in-plane loading conditions. The main novelty of this model is the exploitation of a couple-stress micromechanical approach instead of a classical Cauchy first-order one, for deriving both the homogenized elastic moduli (in the linear range) and the first failure surface for periodic masonry

Couple-stress homogenization has been used for deriving the overall elastic moduli of two-phase composite materials by different authors [44,45], and here is applied to masonry structures within a concurrent multiscale strategy for the first time, to the best authors' knowledge.

The resulting couple-stress continuum for the macroscopic modeling of masonry, usually regarded as a constrained version of the more general Cosserat (or micropolar) continuum model [46,47], in able to account for the size dependence of the deformation behavior usually experienced in heterogeneous materials.

The adoption of a couple-stress model within the proposed multiscale methodology allows for the injection of the characteristic length of masonry in its overall mechanical response in both linear and nonlinear ranges. This potentially leads to an increase in the numerical accuracy with respect to the use of a classical Cauchy macro-continuum, especially in the presence of high strain gradient components of the rotational type.

The proposed couple-stress based multiscale model of masonry has been properly validated, by comparing it with a purely discrete model (regarded as the most accurate one), with reference to the numerical simulation of a shear wall test. The latter model, which takes into account all the microstructural details from the beginning of simulation, is considered as the reference one, but is unreasonable for practical purposes due to its huge computational cost.

2 MULTISCALE/MULTIDOMAIN FRAMEWORK FOR MASONRY AS A PERIODIC COMPOSITE

At the microscopic level, regular brick masonry is modeled as a two-phase periodic composite material, whose constituents are initially perfectly bonded to each other. Since only the in-plane behavior is considered here, this composite is characterized by a periodic microstructure in a 2D setting.

Under these hypothesis, a given masonry structure is represented by a (Cauchy) heterogeneous continuum made of units and mortar joints, occupying a bounded open set $\Omega \subset R^2$. Its external boundary, denoted as $\partial\Omega$ and assumed to be Lipschitz-continuous, is made of two disjoints portions, i.e. $\partial_D\Omega$ and $\partial_N\Omega$, where Dirichlet and Neumann boundary conditions are prescribed, respectively. Moreover, $\partial_D\Omega$ possesses a nonzero measure in order to avoid any arbitrary rigid-body motions (see Fig. 1a). The units (i.e. the bricks) are assumed unbreakable and made of linearly elastic material, whereas the mortar joints, modeled as zero-thickness cohesive interfaces Γ_c placed in between the units, are assumed damageable according to a mixed-mode softening constitutive law accounting for crack initiation and propagation at mortar/brick contact surfaces.

In the quasi-static setting, even under the simplifying assumptions of negligible body forces and small deformations, the response of a masonry structure to general loading conditions can be obtained as the solution of a highly complex nonlinear boundary value problem (BVP), being characterized by a large ratio between structural and brick size.

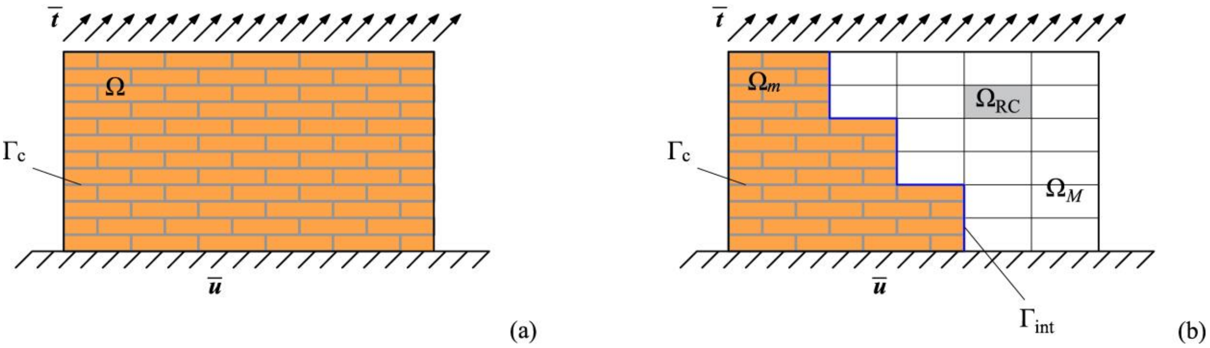

Figure 1: Modeling approaches of regular masonry structures subjected to in-plane loading conditions: (a) microscopic modeling; (b) two-scale multi-domain modeling.

In order to reduce the complexity of such a purely microscopic model, a multiscale strategy is proposed here, based on a two-level domain decomposition technique used in conjunction with a couple-stress homogenization method. The key idea of this strategy consists in using a homogenized model for masonry everywhere, except for properly defined critical regions, collectively referred to as *zone of interest*, where a failure onset criterion is reached. Such a zone includes all the hotspots subjected to incipient cracking (at mortar joints), for which both the assumptions of perfect periodicity and separation of scales needed for correctly applying the above-mentioned homogenization step cease to be valid.

As a consequence, the original single-scale problem is replaced by an equivalent multiscale multi-domain problem, composed of simpler sub-problems involving two well-separated spatial scales (i.e. a couple-stress macroscopic and a Cauchy microscopic models) to be solved in a fully coupled manner. The computational domain Ω is partitioned in two non-overlapping subsets Ω_M and Ω_m, as shown in Fig. 1b. Ω_M is the macroscopic subdomain, on which the (undamaged) homogenized moduli are assigned, whereas Ω_m denotes the microscopic subdomain, representing the zone of interest, for which all the structural details together with the associated microscopic damage phenomena are explicitly accounted for.

Because of this partition, additional internal boundaries are introduced into the model, referred to as micro-to-macro interface and denoted as Γ_{int}. It follows that a new BVP is defined, stated as an interface variational problem which is based on the following Lagrange multiplier formulation: find $(\boldsymbol{u}_m, \boldsymbol{u}_M, \boldsymbol{\lambda}) \in U_m \times U_M \times \Lambda$ such that:

$$
\begin{aligned}
&\int_{\Omega_m/\Gamma_c} \boldsymbol{\sigma}_m \cdot \boldsymbol{\varepsilon}(\delta \boldsymbol{u}_m)\, d\Omega + \int_{\Gamma_c} \boldsymbol{t}(\boldsymbol{u}_m, d) \cdot \delta \boldsymbol{u}_m \, d\Gamma + \int_{\Gamma_{\mathrm{int}}} \boldsymbol{\lambda} \cdot \delta \boldsymbol{u}_m d\Gamma = \int_{\partial_N \Omega_m} \bar{\boldsymbol{t}}_m \cdot \delta \boldsymbol{u}_m d\Gamma, \quad \forall \delta \boldsymbol{u}_m \in V_m \\
&\int_{\Omega_M} \boldsymbol{\sigma}_M \cdot \boldsymbol{\varepsilon}(\delta \boldsymbol{u}_M) + \boldsymbol{\mu}_M \cdot \boldsymbol{\kappa}(\delta \boldsymbol{u}_M)\, d\Omega - \int_{\Gamma_{\mathrm{int}}} \boldsymbol{\lambda} \cdot \delta \boldsymbol{u}_M d\Gamma = \int_{\partial_N \Omega_M} \bar{\boldsymbol{t}}_M \cdot \delta \boldsymbol{u}_M d\Gamma, \quad \forall \delta \boldsymbol{u}_M \in V_M \\
&\int_{\Gamma_{\mathrm{int}}} \delta \boldsymbol{\lambda} \cdot (\boldsymbol{u}_m - \boldsymbol{u}_M)\, d\Gamma = 0, \quad \forall \delta \boldsymbol{\lambda} \in \Lambda
\end{aligned} \qquad ,(1)
$$

where the first two equations are the equilibrium conditions of the portions Ω_m and Ω_M, respectively, and the third one represents the kinematic compatibility condition at the micro-to-macro interface. It is worth noting, here, that the first term of Eq. $(1)_2$ denotes the internal virtual work in the context of couple-stress elasticity.

In Eq. (1), $\boldsymbol{u}_m$ and $\boldsymbol{u}_M$ are the micro- and macro-scale displacement fields, belonging to the spaces of admissible solutions, U_m and U_M, respectively, whereas $\delta\boldsymbol{u}_m$ and $\delta\boldsymbol{u}_M$ denote the corresponding virtual fields, belonging to the spaces of test functions, V_m and V_M, respectively. Moreover, $\bar{\boldsymbol{t}}_m$ and $\bar{\boldsymbol{t}}_M$ are the restrictions of $\bar{\boldsymbol{t}}$ to the portions $\partial_N\Omega_m$ and $\partial_N\Omega_M$ of $\partial_N\Omega$ (see Fig. 1b), whereas $\boldsymbol{\lambda}$ denotes the unknown Lagrange multiplier field and $\delta\boldsymbol{\lambda}$ its arbitrary variation, belonging to the same space Λ, usually referred to as space of Lagrange multipliers. Then, $\boldsymbol{\varepsilon}$ and $\boldsymbol{\kappa}$ denote the strain and curvature operators, respectively, the second one being defined only for the (couple-stress) macroscopic model of masonry. Finally, the macroscopic stress $\boldsymbol{\sigma}_M$ and couple-stress $\boldsymbol{\mu}_M$ tensors are related to the macroscopic strain $\boldsymbol{\varepsilon}(\boldsymbol{u}_M)$ and curvature $\boldsymbol{\kappa}(\boldsymbol{u}_M)$ tensors via a suitably identified constitutive law, resulting from the couple-stress based homogenization explained in Section 2.2.

2.1 Microscopic modeling of masonry

In the present multiscale model, masonry is described as a heterogeneous Cauchy continuum at the microscopic scale, only within the zone of interest, i.e. the region where all the nonlinearities due to damage initiation and evolution are assumed to occur. The so-called simplified micro-modeling is chosen for describing the microscopic response of masonry, meaning that artificially expanded units are modeled by bulk elements whereas the behavior of mortar joints is lumped into zero-thickness interface elements placed in between the units. It is worth recalling here that units are assumed to be unbreakable, such an approach is able to account for only mixed-mode cracking of mortar joints (and eventually masonry crushing), but cannot describe any vertical or diagonal tensile cracking of bricks.

Therefore, all the joints are equipped with an intrinsic mixed-mode cohesive law, involving a scalar state variable D indicating the current interface damage level (the value 0 indicates a perfect interface, whereas the value 1 is associated with a completely failed interface). A modified version of the cohesive law described in [48] is used here, where an additional compressive cap is introduced in order to correctly represent the so-called masonry crushing phenomena. It is worth noting that, unlike the tensile response, the compressive one is assumed to be reversible. This approximation, which is valid in the absence of unloading after the initiation of masonry crushing, allows us to avoid the introduction of damage variables that take into account the entire compressive deformation history. The elastic and inelastic material parameters of the nonlinear springs representing the mortar joints are: normal, K_n, and tangential, K_s, elastic stiffness parameters, tensile, f_t, and shear, c, cohesive strengths, (masonry) compressive strength, f_c, friction angle, ϕ, and both mode-I, $G_{\mathrm{I}c}$, and mode-II, $G_{\mathrm{II}c}$, fracture energies. The elastic stiffness parameters of the interface are not intended as penalty values, but have a precise physical meaning, being derived from the properties of both masonry constituents and the joint thickness, according to the approach followed in [49].

2.2 Macroscopic modeling of masonry

Outside the zone of interest, a couple-stress model is used for representing masonry at the macroscopic scale. The couple-stress theory can be considered as a special case of the second gradient model for which only the effect of the gradient of the material rotation (or macro-rotation), i.e. the skew-symmetric part of the displacement gradient, is taken into account [44,45]. Alternatively, this theory can be regarded as a constrained version of more general Cosserat theory, in which the micro-rotation (treated as independent degree of freedom in unconstrained Cosserat theory [46,47]) is equal to the macro-rotation.

The main feature of the couple-stress model is the presence of additional work-conjugated stress and strain measures, i.e. the couple-stress $\bar{\boldsymbol{\mu}}$ and the curvature $\bar{\boldsymbol{\kappa}}$ tensors, respectively.

The overall (i.e. macroscopic) behavior of the undamaged brick masonry modeled as a couple-stress continuum is here obtained via a Cauchy/couple-stress homogenization technique under plane stress assumptions. To this end, a proper repeating cell (RC) is defined, which is representative of the given periodic microstructural arrangement. In the case of classical running bond, the most commonly adopted RC is that shown in Fig. 2a.

As a preliminary step of the above-mentioned homogenization scheme, the (Cauchy) microscopic displacement field $\boldsymbol{u} = (u_1, u_2)^T$ can be expressed as the superposition of a quadratic part and a fluctuation field $\boldsymbol{w} = (w_1, w_2)^T$, as follows [50]:

$$\begin{aligned} u_1 &= \bar{\varepsilon}_{11} x_1 + \bar{\varepsilon}_{12} x_2 - \bar{\kappa}_{31} x_1 x_2 - \frac{\bar{\kappa}_{32}}{2} x_2^2 + w_1\left(x_1, x_2\right) \\ u_2 &= \bar{\varepsilon}_{12} x_1 + \bar{\varepsilon}_{22} x_2 + \bar{\kappa}_{32} x_1 x_2 + \frac{\bar{\kappa}_{31}}{2} x_1^2 + w_2\left(x_1, x_2\right) \end{aligned}, \qquad (2)$$

where $\bar{\varepsilon}_{11}$, $\bar{\varepsilon}_{22}$ and $\bar{\varepsilon}_{12}$ are the Cauchy macroscopic strains, $\bar{\kappa}_{31}$ and $\bar{\kappa}_{32}$ are the macroscopic (bending) curvatures of an effective couple-stress medium, whereas x_1 and x_2 are the local coordinates of a centered Cartesian system aligned with the orthotropic axes of the RC, as shown in Fig. 2b.

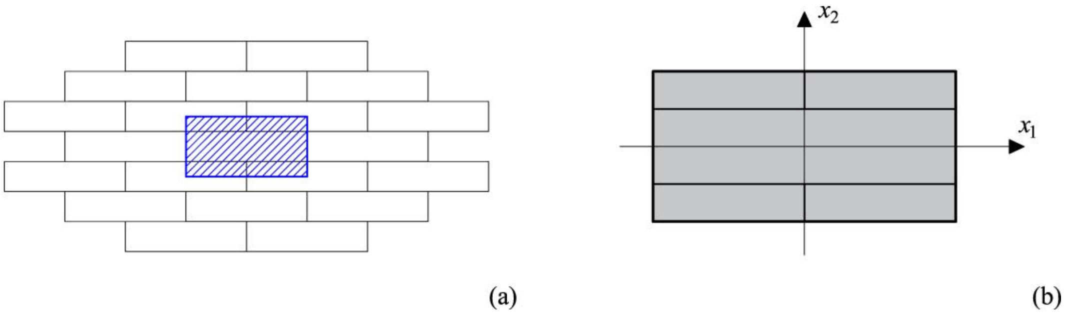

Figure 2: Couple-stress homogenization of running bond masonry: (a) adopted repeating cell (RC); (b) local coordinate system for the microscopic field description.

In order to derive the macroscopic moduli of masonry, five different microscopic BVPs are solved over the given RC, corresponding to the pure (three Cauchy and two bending) macro-deformation modes (see Fig. 3). Periodic fluctuations are applied for the Cauchy deformation modes, whereas the special mixed boundary conditions used in [51] are imposed for the bending deformation modes. These boundary conditions involve a combination of periodic, antiperiodic and zero fluctuation on different portions of the RC boundary, as shown in Fig. 4.

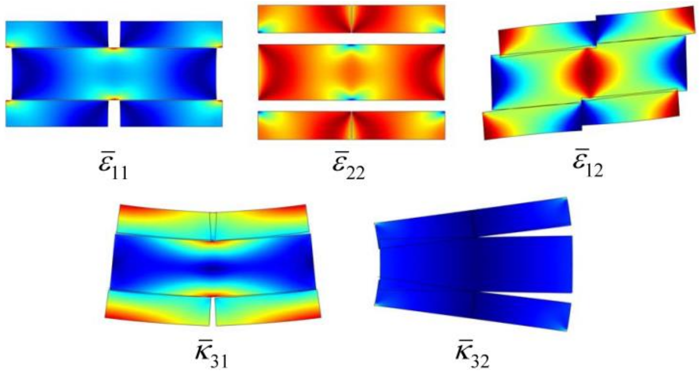

Figure 3: Pure macroscopic deformation modes for the couple-stress homogenization.

In fact, as argued in [52], there in general no reason for assuming a periodicity requirement on the fluctuation field in the presence of overall bending curvatures.

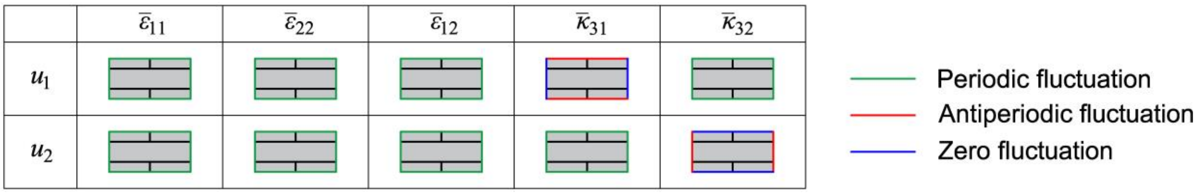

Figure 4: Boundary conditions required for the couple-stress homogenization of masonry.

Due to the assumed orthotropic nature of the masonry microstructure, only six overall elastic moduli have to be identified via the proposed Cauchy/Couple-Stress homogenization. The complete homogenized constitutive law for masonry written in matrix form reads as follows:

$$\begin{bmatrix} \bar{\sigma}_{11} \\ \bar{\sigma}_{22} \\ \bar{\sigma}_{12} \\ \bar{\mu}_{31} \\ \bar{\mu}_{32} \end{bmatrix} = \begin{bmatrix} \bar{A}_{1111} & \bar{A}_{1122} & 0 & 0 & 0 \\ \bar{A}_{1122} & \bar{A}_{2222} & 0 & 0 & 0 \\ 0 & 0 & \bar{A}_{1212} & 0 & 0 \\ 0 & 0 & 0 & \bar{C}_{3131} & 0 \\ 0 & 0 & 0 & 0 & \bar{C}_{3232} \end{bmatrix} \begin{bmatrix} \bar{\varepsilon}_{11} \\ \bar{\varepsilon}_{22} \\ \bar{\varepsilon}_{12} \\ \bar{\kappa}_{31} \\ \bar{\kappa}_{32} \end{bmatrix}, \tag{3}$$

where $\bar{\sigma}_{ij}$ and $\bar{\varepsilon}_{ij}$ (i,j = 1,2) are the classical macroscopic stress and strain components, respectively; $\bar{A}_{ijhk}$ (i,j,k,h = 1,2) are the classical overall moduli; $\bar{\mu}_{3i}$ and $\bar{\kappa}_{3i}$ (i = 1,2) are the couple-stress and curvature components, respectively; $\bar{C}_{3i3i}$ (i = 1,2) are the bending moduli, responsible for the introduction of a length scale parameter, intimately related to the brick size.

3 DESCRIPTION OF THE MULTISCALE SIMULATION ALGORITHM

In this section, the proposed multiscale simulation algorithm is illustrated, together with the related computational details. It is worth recalling here that the proposed multiscale procedure belongs to the class of *adaptive model refinement* methods, so named by analogy with the most used *adaptive model refinement* methods. The key feature of the present algorithm consists in replacing the homogenized macroscopic model by the original microscopic model after a properly defined zooming-in criterion is satisfied, in an automatic matter during the simulation. Such a criterion essentially is a microscopically derived first failure criterion for the homogenized masonry. To this end, coherently with the adopted homogenization scheme, a couple-stress first failure surface has to be constructed for the given RC prior to the multiscale simulation, according to the procedure discussed in Section 3.1.

At the beginning, the computational domain is partitioned in a finite number of coarse-scale finite elements (called *macro-elements*) whose size coincides with that of the considered repeating cell (see Fig. 5a). In other words, there exists a unique link between a model parameter (i.e. the microstructural characteristic size) and a numerical parameter (i.e. the macroscopic mesh element size), analogously to what is assumed in the so-called couple-volume approach [53]. It is worth noting here that the presence of macro-elements cut by the external boundaries of the computational domain is not allowed in the present multiscale strategy, due to the fact that the couple-stress overall first failure strengths are related to the internal length of the microstructure and thus to the entire cell size. As a consequence, cut macro-elements are suitable replaced with the underlying microstructure in the pre-processing step.

At a given load step, the macro-elements for which the zooming-in criterion is satisfied are flagged as critical, and replaced by finely meshed repeating cells, as shown in Fig. 5b. Such a model refinement operation is repeated during the simulation within an incremental-iterative strategy until the final collapse occurs or the maximum number of load increments is reached (see Fig. 5c).

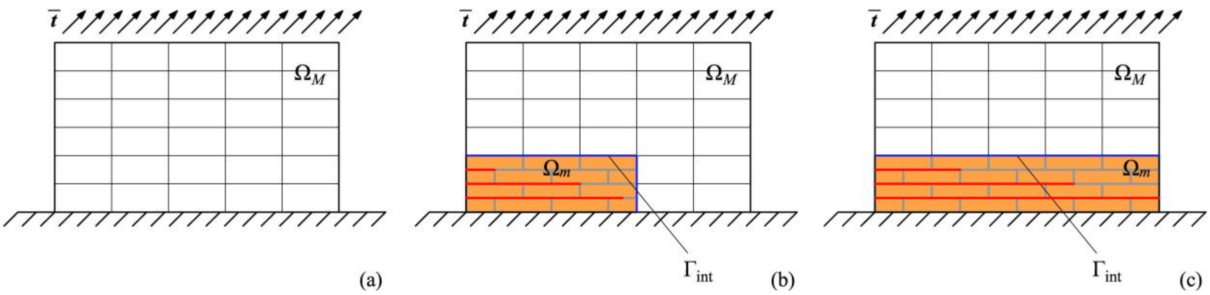

Figure 5: Schematic representation of the adaptive model refinement strategy: (a) initial coarse mesh composed of homogenized macro-elements; (b) intermediate multi-level mesh with partial structural damage; (c) final multi-level mesh at incipient collapse.

The above-described adaptive model refinement algorithm has been implemented within the commercial finite element simulation environment COMSOL Multiphysics® [54], by exploiting its versatile scripting capabilities in MATLAB® language. The built-in quasi-static continuation solver has been employed in order to perform displacement-controlled nonlinear analyses, equipped with an additional stop condition responsible for verifying the satisfaction of the above-mentioned zooming-in criterion for all the macro-elements in the current model. The progressive update of the computational model (including geometry, mesh and micro-to-macro boundary conditions) is made possible by adding to the standard Newton-Raphson loop a further model refinement loop performed via a dedicated MATLAB® code linked to the adopted simulation environment.

3.1 Couple-stress first failure locus for masonry

The main ingredient of the proposed adaptive concurrent multiscale model is the *first failure locus*, formulated for a perfectly periodic masonry subjected to arbitrary quasi-static macroscopic loading paths, initially proposed for a Cauchy macro-continuum (see [42,43]) and here extended to a couple-stress homogenized model. Such a locus is defined for a given masonry repeating cell under plane stress assumptions, as the set of macroscopic strain states corresponding to the microscopic crack onset in the most stressed point along the cohesive interfaces. From a numerical point of view, the first failure locus is derived by interpolating the failure points obtained considering a finite subset of macrostrain paths.

The boundary conditions assumed for the repeating cell subjected to the mixed macrostrain paths are not coinciding with those employed for pure macrostrain path directions (sketched in Fig. 4). As a matter of fact, the actual boundary conditions to be used for mixed loading paths are not known in the literature, to the best of the authors' knowledge. For the sake of simplicity, an approximate approach has been pursed in the present work, by which the microscopic fluctuation field associated with a given macrostrain path direction is expressed as the linear combination of the five microscopic fluctuation fields associated with the pure macrostrain paths, by exploiting the linearity of the mechanical response up to failure. It follows that the resulting microscopic stress and strain fields are simply obtained by combining those pertaining to the three Cauchy and two couple-stress modes, by adopting the same combination coefficients used for the prescribed macroscopic strain field. It is worth noting that this simplified approach provides exact results only in the case of pure macrostrain path directions and in the absence of bending contributes (for which periodic boundary conditions are always valid).

Given a suitable angular coordinate system (ϕ_1, ϕ_2, ϕ_3, ϕ_4) defined over the 5-dimensional couple-stress macrostrain space, any point representing a given macrostrain state can be expressed as follows:

$$\begin{aligned}
\bar{\kappa}_{31} &= \lambda \cos\phi_1 \\
\bar{\kappa}_{32} &= \lambda \sin\phi_1 \cos\phi_2 \\
\bar{\varepsilon}_{12} &= \lambda \sin\phi_1 \sin\phi_2 \cos\phi_3 \\
\bar{\varepsilon}_{11} &= \lambda \sin\phi_1 \sin\phi_2 \sin\phi_3 \cos\phi_4 \\
\bar{\varepsilon}_{22} &= \lambda \sin\phi_1 \sin\phi_2 \sin\phi_3 \sin\phi_4
\end{aligned} \quad , \tag{4}$$

λ being the loading parameter which controls the magnitude of the prescribed macrostrain. The considered set of loading directions covers the ranges $0 \leq \phi_1, \phi_2, \phi_3 \leq 180°$ and $-180° \leq \phi_4 \leq 180°$. For each macrostrain path direction, the critical load factor λ_c can be easily computed in the post-processing step, by exploiting the linearity of the interface constitutive law up to this value. As the first failure locus is expected to be non-smooth, it must be discretized in a fine manner, in order to accurately compute the critical load factor even in the neighborhood of corner points. Such a fine discretization can be reached by choosing always very small angular increments.

3.2 Computational details

As already stated, the macroscopic behavior of masonry is represented by a couple-stress continuum modeling, whose elastic properties have been properly identified. Within a standard finite element setting, such a modeling is directly derived from an unconstrained Cosserat modeling, in which displacements and rotations are taken as independent nodal variables, thus avoiding the higher order continuity requirement typical of pure displacement formulations. The additional internal constraint enforcing the equality between micro- and macro-rotations is introduced in the variational formulation by means of the penalty approach proposed in [55].

Due to the presence of both coarse- and fine-scale discretizations in the same model, a non-conforming mesh at the double-sided micro-to-macro interface Γ_{int} necessarily appears, characterized by the presence of nonmatching nodes, referred to as "hanging nodes", at the microscopic side of this interface. The displacement continuity along Γ_{int} is enforced pointwise by using a Linear Multi-Point Constraint approach, resulting in a strong coupling between micro- and macro-displacements [56]. Furthermore, the micro-rotations at the macroscopic side of the interface are kept free in the present approach. In fact, there is no need of restraining them, due to the presence of the above-mentioned internal constraint, introduced to (approximately) enforce the couple-stress kinematics. It is worth noting here that the adopted coupling technique automatically enforces any crack opening at the micro-to-macro interface to be suppressed, thus allowing no damage percolation outside the zone of interest, coherently with the basic assumptions of the model.

4 NUMERICAL SIMULATIONS: THE SHEAR WALL TEST

In this section, the proposed couple-stress based adaptive multiscale strategy has been validated, with reference to the failure analysis of a masonry wall subjected to a shear test. Such a test, introduced in [57], has been chosen as an example of brick masonry exhibiting a complex in-plane shear-flexure behavior, which is typical of real-life traditional structures subjected to seismic actions.

4.1 Description of the test specimen and the boundary conditions

The test specimen here employed for assessing the validity of the proposed multiscale method is the small-sized wall shown in Fig. 6. Its dimensions are L = 980 mm and H = 1106 mm, with a resulting width-to-height ratio of about one. The wall presents a central opening of 220 × 372 mm^2. The loading history is made of two steps. In the first one, a confinement is applied by prescribing a vertical displacement of the wall top until a compressive stress of 0.30 MPa is reached in average. In the second one, a top horizontal displacement is monotonically increased in a confined way, i.e. by blocking both the rotation and the vertical displacement of the wall top. The overall horizontal reaction force is found as the summation of nodal forces computed at all the nodes belonging to the top constrained edge.

The wall is made of bricks of 210 × 52 × 100 mm^3 periodically arranged according to a running bond pattern. The thickness of mortar joints is equal to 10 mm. The elastic behaviors of both brick and mortar materials are assumed linearly elastic and isotropic, whose material constants, i.e. Young's moludus E and Poisson's ratio v, are listed in Table 1. The associated inelastic parameters, i.e. the tensile f_t and shear c cohesive strengths, the (masonry) compressive strength f_c, the friction angle ϕ, and the mode-I G_{Ic} and mode-II G_{IIc} fracture energies, taken as in [58], are listed in Table 2.

4.2 Results of the multiscale numerical simulation (MNS)

As a preliminary step needed for the subsequent multiscale analysis, the homogenized moduli for the given masonry have been derived under the assumption of plane stress state, as explained in Section 2.2. The obtained overall moduli are listed in Table 3. The adopted finite element discretization consists in a sufficiently refined mapped mesh whose size is 2 mm.

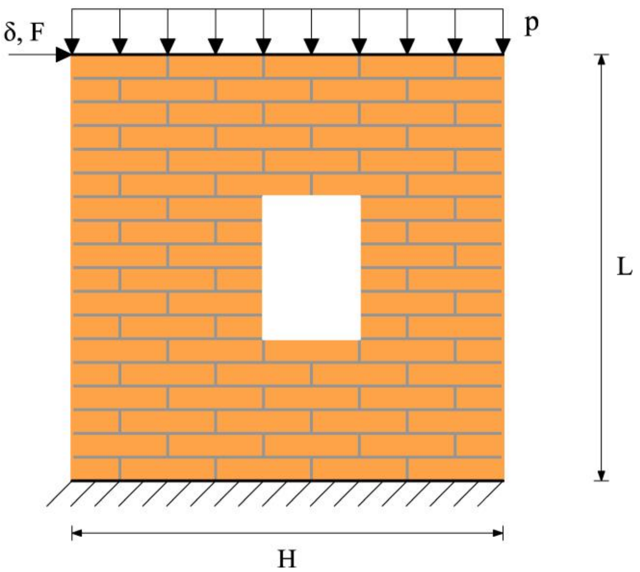

Figure 6: Masonry wall subjected to a shear test: geometry and boundary conditions.

Component	E [MPa]	ν [-]
Brick	16,700	0.15
Mortar	782	0.14

Table 1: Elastic material properties of bricks and mortar joints.

f_t [MPa]	c [MPa]	f_c [MPa]	ϕ [deg]	G_{Ic} [N/mm]	G_{IIc} [N/mm]
0.25	0.35	10.5	36.9	0.018	0.125

Table 2: Inelastic material parameters of mortar joints.

$\bar{A}_{1111}$ [MPa]	$\bar{A}_{2222}$ [MPa]	$\bar{A}_{1122}$ [MPa]	$\bar{A}_{1212}$ [MPa]	$\bar{C}_{3131}$ [MN]	$\bar{C}_{3232}$ [MN]
9983.4	3935.9	404.20	3054.7	6.3357	6.5059

Table 3: Homogenized moduli for the undamaged masonry modeled as a couple-stress macro-continuum.

Using the same RC and the same mesh as for the determination of the homogenized moduli, the first failure surface has been also derived, according to the methodology illustrated in Section 3.1. In practice, several (linear) microscopic problems have been solved for different macroscopic strain directions, each of which is associated with a critical point of this locus. Each critical point represents the macrostrain state corresponding to the occurrence of the first nonlinearity in the cohesive response of mortar joints. A constant increment of 2° for the angular coordinates has been chosen, in order to obtain a sufficiently accurate representation of this locus.

Since this numerically derived locus is defined over a 5-dimensional space, it may be effectively represented as a family of contour graphs. For the sake of clarity, only the contour lines obtained as the intersection of the locus with the coordinate planes are depicted in Fig. 7.

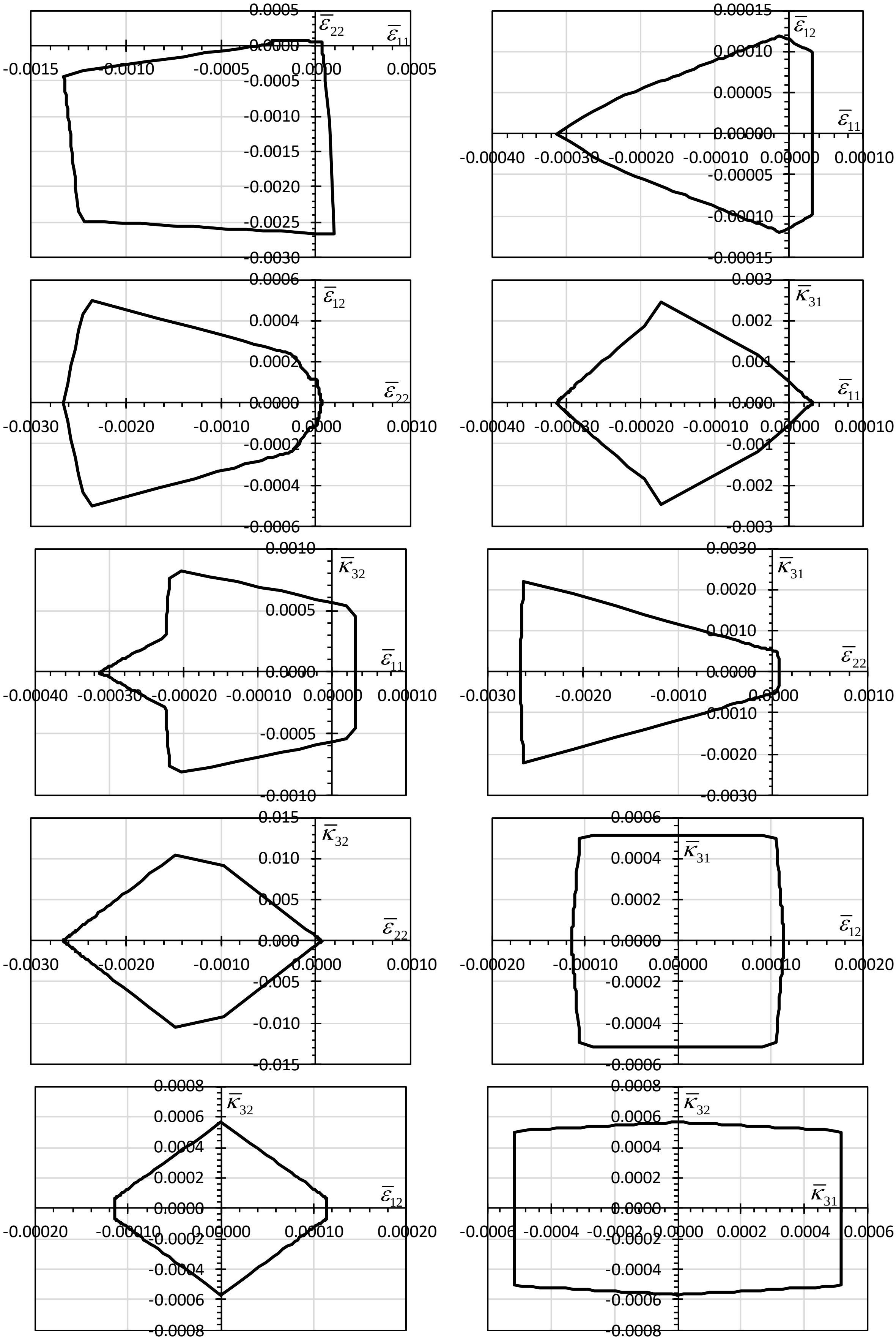

Figure 7: Contour representation for the microscopically informed first failure surface of regular masonry.

The multiscale numerical simulation (MNS) has been conducted by using the algorithm described in Section 3. Fig. 8 shows the structural response for the shear wall test obtained via MNS, in terms of load-displacement curve. This response presents an initial quasi-linear behavior followed by a nonlinear hardening branch. A load peak of about 43 kN is found, after which a moderate softening branch can be identified. It is worth noting here that the multiscale analysis has experienced some convergence issues due to the adopted displacement control continuation method.

By more closely analyzing the structural response shown in Fig. 8, a number of discontinuity points can be detected, which can be attributed to the superposition of homogenization and micro-to-macro coupling errors. These errors, unlike discretization ones, cannot be controlled during the adaptive model refinement step via the proposed multiscale methodology. These errors are associated with a non-negligible delay for micro-crack nucleation and propagation in the neighborhood of the micro-to-macro interface and potentially lead to the loss of validity of the numerical simulation. To this end, the following a posteriori error is introduced:

$$e_F = \frac{F_{\text{pred}} - F_{\text{corr}}}{F_{\text{corr}}} \times 100, \tag{5}$$

defined as the percent variation in the applied force before (F_{pred}) and after (F_{corr}) the iterative correction associated with adaptive model refinement within each load incremental step. The maximum value attained for this error during the multiscale numerical simulation is of about 4%, thus confirming the validity of the proposed approach.

Fig. 8 shows also the deformed configurations of the multiscale model for three different incremental steps, associated with increasing extensions of the zone of interest. In this zone, a damage variable map is added, in order to present a deeper insight into the mechanical behavior of mortar joints during the simulation. In detail, the coarse-level elements outside the zone of interest are shaded in grey, whereas the damage variable defined on the cohesive interfaces ranges from 0 (blue) to 1 (red).

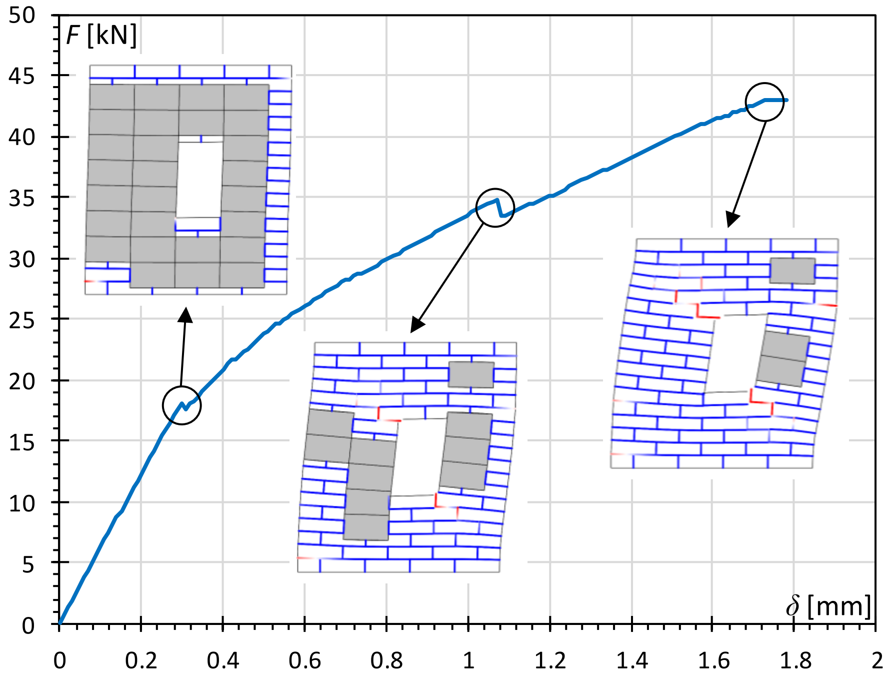

Figure 8: Force vs displacement curve obtained from the multiscale numerical simulation (MNS).

4.3 Comparisons with direct numerical simulation (DNS) and experiments

In order to illustrate the effectiveness of the multiscale numerical simulation (MNS), the previously presented results have compared with those coming from a direct numerical simulation (DNS), here considered as the reference ones, and from some experimental data found in the literature.

In Fig. 9, the comparison between MNS and DNS is shown in terms of force versus displacement curve. It is worth noting that a direct numerical simulation (DNS), for which all the microstructural details are explicitly taken into account from the beginning, is usually very costly for the complete failure analysis of masonry structures, especially for larger ones, and its only advantage consists in a very high accuracy. The proposed multiscale methodology is able to obtain a structural response which is almost superposed to that resulting from the DNS, in particular in the neighborhood of the peak load. It follows that the carrying capacity of masonry is well predicted, as confirmed by the very small percentage error on the peak load between the two analyses (less than 1%).

Fig. 9 also shows the comparison of the present results with the experimental ones found in [57]. The numerically predicted response of the masonry wall is very close to the measured one, but the overall stiffness appears to be slightly overestimated probably due to the fact that brick are here assumed unbreakable. On the other hand, the predicted peak load is lower than the experimental one, with a percentage error of about 8%. This provides a further confirmation of the validity of the proposed numerical methodology.

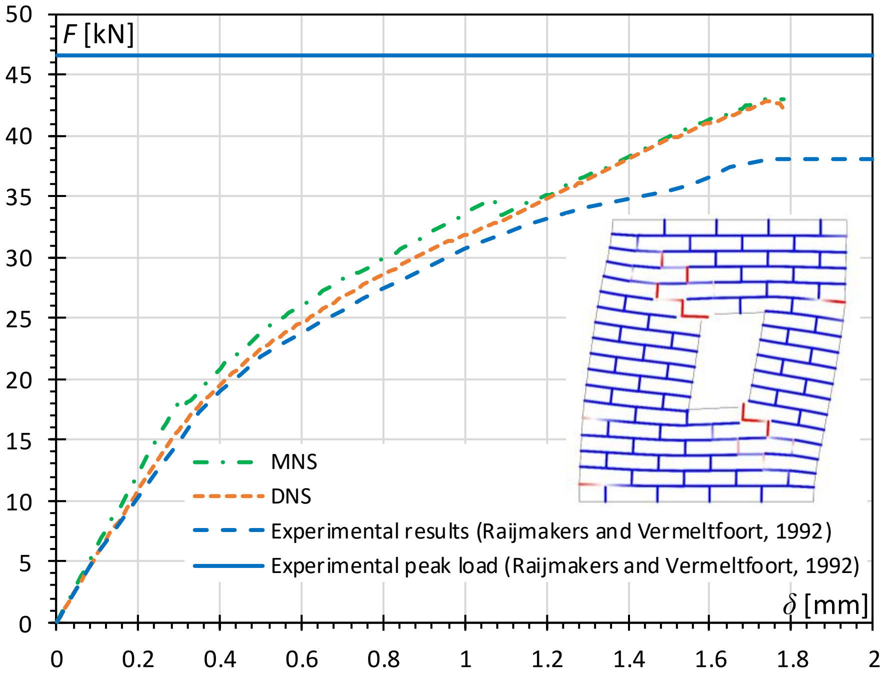

Figure 9: Comparison in terms of force vs displacement curve among multiscale numerical simulations (MNS), direct numerical simulation (DNS), and experiments by Raijmakers and Vermeltfoort [57].

	δ = 0.10 mm	δ = 0.80 mm	δ = 1.75 mm
DNS (reference)	1,060,460	8,483,680	18,558,050
MNS (present)	65,110	1,792,198	6,414,300

Table 4: Number of cumulative DOFs for MNS and DNS, computed at three different incremental steps.

Finally, the computational performances exhibited by the proposed multiscale algorithm have been investigated. These performances have been measured by monitoring the cumulative number of total degrees of freedom (DOFs) over the incremental steps of simulation, for the multiscale (MNS) and direct (DNS) numerical simulations, as shown in Table 4. It is worth noting that, whereas the number of DOFs remains constant in the DNS, the number of DOFs rapidly increases in the MNS as the zone of interest is progressively enlarged. The resulting cumulative DOF ratio between MNS and DNS is of about 35% is obtained.

The associated CPU time ratio between MNS and DNS is of about 47%, corresponding to a significant speed-up value. Nevertheless, it is believed that the efficiency of the proposed multiscale method is not fully exploited, since the computational cost could be further reduced by adopting a more efficient communication between the MATLAB scripting code and COMSOL Multiphysics finite element environment.

4.4 Investigation of the role of bending deformation effects on the multiscale failure analysis

The proposed multiscale approach is regarded as a generalization of the approach proposed in [42], obtained by including the effect of bending deformations modes on both the overall moduli tensor and the first failure surface of masonry. In order to better investigate the role of these effects, a comparison between the present model, denoted as CSM2 (Couple-Stress Multiscale/Multidomain) model, and the original model, denoted as CM2 (Cauchy Multiscale/Multidomain), is presented here.

This comparison is shown in terms of force-displacement curves obtained via these two approaches (see Fig. 10). It can be noted that the apparent stiffness in the linear range is correctly predicted by both models, confirming that the size effect related to bending behavior is not relevant in the linear response of the considered masonry structure.

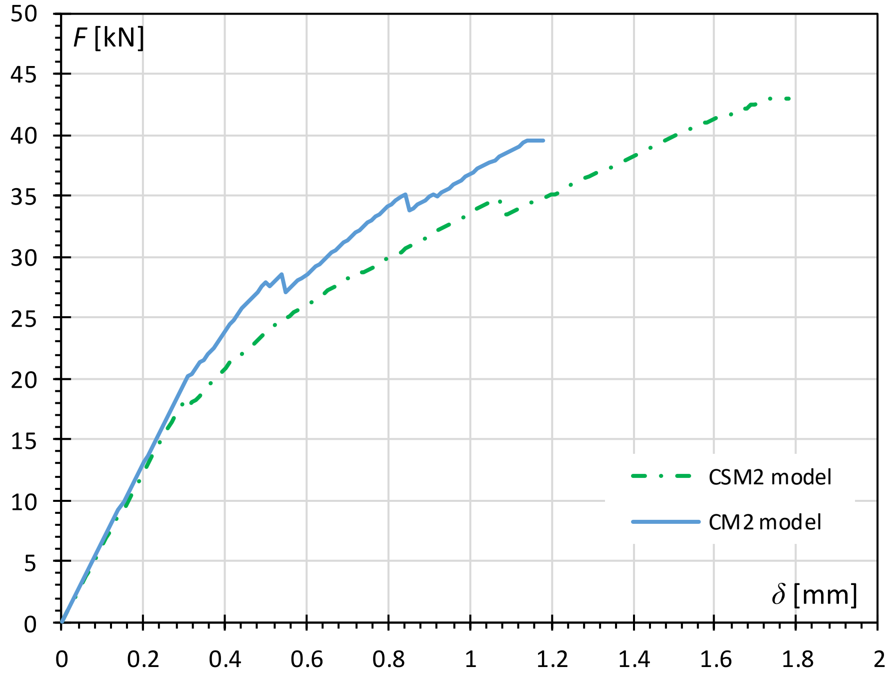

Figure 10: Comparison in terms of force vs displacement curve between the present model (Couple-Stress Multiscale/Multidomain or CSM2) and the model proposed in [42] (Cauchy Multiscale/Multidomain or CM2).

Conversely, considering explicitly the bending deformation modes in the mechanical behavior of homogenized masonry has a direct influence on the predicted overall structural response in the nonlinear range. In particular, the response predicted by the previously proposed multiscale approach based on a (micro/macro) Cauchy/Cauchy homogenization is stiffer than that obtained via the present (micro/macro) Cauchy/Couple-Stress homogenization.

These numerical results can be easily explained, by observing that the Cauchy-based first failure criterion is less restrictive than the newly proposed Couple-Stress based one. This means that the CM2 approach inevitably leads to a delay of the zooming-in operations with respect to the CSM2 approach, and thus to an artificial damage arrest in the neighborhood of the micro-to-macro interface.

In summary, the proposed enhanced multiscale methodology is able to better predict the stress redistribution during the microscopic damage propagation, and ultimately to derive a more accurate estimate of both carrying capacity and ductility properties of masonry structures.

5 CONCLUSIONS

A Couple-Stress/Cauchy multiscale approach has been proposed for the nonlinear analysis of periodic masonries under in-plane loading conditions. Such an approach relies on a two-scale domain decomposition method, used in conjunction with an adaptive model refinement technique, able to zoom the masonry zones undergoing microscopic damage initiation in an automatic manner.

Model adaptivity is a fundamental ingredient of the present multiscale strategy, because it highly affects the overall computational cost of the numerical simulations. The main novelty of the present work consists in using as zooming-in criterion a microscopically derived first failure criterion for the homogenized masonry in the framework of couple-stress elasticity. In fact, unlike the criteria proposed in the previous works [42,43] by some of the authors, the new approach explicitly takes into account the effect of bending macro-deformation modes on the damage onset at mortar joints as well as on the homogenized elastic moduli.

The present multiscale model has been suitably validated by applying it for the numerical derivation of the structural response of a masonry wall subjected to a shear wall test. The results obtained via the proposed multiscale numerical simulation (MNS) have been compared with those coming from both a direct numerical simulation (DNS) and experiments found in the literature. The MNS has been found to predict very accurately both the peak and the post-peak responses. In detail, the error on the peak load has been found to be very small (less than 1%). The high level of accuracy obtained in the MNS is essentially due to the fact that no simplifications in the structural behavior beyond the elastic limit of the masonry material have been made, thus allowing an accurate evaluation of damage evolution under complex loading paths.

As far as the computational performances exhibited by the proposed model is concerned, the number of cumulative DOFs during the MNS has been monitored. A multiscale to direct DOF ratio of about 0.35 has been found, associated with a rather good speed-up value (about 47%). This value is specific for the considered structural application, and is susceptible to be reduced for other applications involving a more localized damage evolution.

Finally, the proposed multiscale methodology based on a couple-stress homogenization approach has been shown to better predict the carrying capacity of masonry structures with respect to existing approaches based on a classical (Cauchy) first-order homogenization, confirming the importance of explicitly taking in account the (bending) higher-order deformation effects on the homogenized response of masonry material.

Encouraged by the present numerical results, the following improvements of the present strategy could be object of future investigations.

Firstly, the proposed multiscale algorithm could be extended to more general loading and failure modes, in order to incorporate the so-called out-of-plane failure mechanisms, whose investigation still represents an open issue in the current research. The main differences could be the adoption of 3D or shell finite elements (for both bulk and interfaces), and, thus, the computation of additional homogenized moduli, as well as of more complex first failure surfaces incorporating also the influence of out-of-plane deformation modes on the masonry's strength. In particular, the use of shell finite elements could improve the computational efficiency of the multiscale model, but requires the development and implementation of new Cosserat-type shell elements into the adopted simulation environment, involving extra degrees of freedom for the in-plane behavior (which is valid only in the case of blocks laid as stretchers).

Secondly, the present multiscale strategy could be used for investigating the so-called size effects in masonry structures usually experienced in both linear and nonlinear ranges. In detail, the incorporation of a characteristic length via the proposed couple-stress homogenized model should be able to predict the different behaviors exhibited by small- and large-sized masonries, characterized by significant variations of the ratio between microstructural and overall sizes.

Thirdly, a more sophisticated multiscale model could be developed, able to capture the influence of higher-order deformation modes on both linear and nonlinear ranges of the structural response of masonry subjected to arbitrary loading conditions. Such a model should be based on the synergistic application of both concepts of *scale transition* and *scale embedding*, eventually exploiting a new multiscale method based on a two-step homogenization involving three scales of interest (i.e. micro/meso/macro-scales), as recently proposed in [59] for ceramic matrix composites. The introduction of a further intermediate scale of observation (i.e. the mesoscopic scale) should increase the overall accuracy in predicting the structural behavior of masonry, especially in the presence of severe strain localization phenomena.

ACKNOWLEDGMENTS

This work is supported by Italian Ministry of University and Research (P.R.I.N. National Grant 2015, B86J16002300001; Sapienza and Calabria Research Units) and by Sapienza University Grant 2016, B82F16005920005.

REFERENCES

[1] B. Chetouane, F. Dubois, M. Vinches, C. Bohatier, NSCD discrete element method for modelling masonry structures, *International Journal for Numerical Methods in Engineering*, **64**, 65-94, 2005.

[2] J.V. Lemos, Discrete Element Modeling of Masonry Structures, *International Journal of Architectural Heritage*, **1**, 190-213, 2007.

[3] D. Baraldi, E. Reccia, A. Cazzani, A. Cecchi, Comparative analysis of numerical discrete and finite element models: The case of in-plane loaded periodic brickwork, *Composites: Mechanics, Computations, Applications*, **4**(4), 319-344, 2013.

[4] D. Baraldi, E. Reccia, A. Cecchi, In plane loaded masonry walls: DEM and FEM/DEM models. A critical review, *Meccanica*, 1-16, 2017.

[5] P.B. Lourenco, Computations on historic masonry structures, *Progress in Structural Engineering and Materials*, **4**, 301-319, 2002.

[6] C. Calderini, S. Cattari, S. Lagomarsino, In-plane strength of unreinforced masonry piers, *Earthquake Engineering and Structural Dynamics*, **38**, 243-267, 2009.

[7] M. Valente, G. Milani, Seismic assessment of historical masonry towers by means of simplified approaches and standard FEM, *Construction and Building Materials*, **108**, 74-103, 2016.

[8] L. Ascione, L. Feo, F. Fraternali, Load carrying capacity of 2D FRP/strengthened masonry structures, *Composites Part B: Engineering*, **36**(8), 619-626, 2005.

[9] A. Caporale, L. Feo, D. Hui, R. Luciano, Debonding of FRP in multi-span masonry arch structures via limit analysis, *Composite Structures*, **108**, 856-865, 2014.

[10] F.G. Carozzi, G. Milani, C. Poggi, Mechanical properties and numerical modeling of Fabric Reinforced Cementitious Matrix (FRCM) systems for strengthening of masonry structures, *Composite Structures*, **107**, 711-725, 2014.

[11] A. D'Ambrisi, F. Focacci, A. Caporale, Strengthening of masonry-unreinforced concrete railway bridges with PBO-FRCM materials, *Composite Structures*, **102**, 193-204, 2013.

[12] L. Feo, R. Luciano, G. Misseri, L. Rovero, Irregular stone masonries: Analysis and strengthening with glass fibre reinforced composites, *Composites Part B: Engineering*, **92**, 84-93, 2016.

[13] A. Garofano, F. Ceroni, M. Pecce, Modelling of the in-plane behaviour of masonry walls strengthened with polymeric grids embedded in cementitious mortar layers, *Composites Part B: Engineering*, **85**, 243-258, 2016.

[14] A. Monaco, G. Minafò, C. Cucchiara, J. D'Anna, L. La Mendola, Finite element analysis of the out-of-plane behavior of FRP strengthened masonry *panels*, *Composites Part B: Engineering*, **115**, 188-202, 2017.

[15] G.P. Lignola, C. Caggegi, F. Ceroni, S. De Santis, P. Krajewski, P.B. Lourenço, M. Morganti, C. (Corina) Papanicolaou, C. Pellegrino, A. Prota, L. Zuccarino, Performance assessment of basalt FRCM for retrofit applications on masonry, *Composites Part B*: *Engineering*, **128**, 1-18, 2017.

[16] M. Malena, F. Focacci, C. Carloni, G. de Felice, The effect of the shape of the cohesive material law on the stress transfer at the FRP-masonry interface, *Composites Part B: Engineering*, **110**, 368-380, 2017.

[17] P.B. Lourénço, R. De Borst, J.G. Rots, A plane stress softening plasticity model for orthotropic materials, *International Journal for Numerical Methods in Engineering*, **40**, 4033-4057, 1997.

[18] L. Berto, A. Saetta, R. Scotta, R. Vitaliani, An orthotropic damage model for masonry structures, *International Journal for Numerical Methods in Engineering*, **55**, 127-157, 2002.

[19] L. Pelà, M. Cervera, P. Roca, Continuum damage model for orthotropic materials: application to masonry, *Computer Methods in Applied Mechanics and Engineering*, **200**(9-12), 917-030, 2011.

[20] A. Anthoine, Derivation of the in-plane elastic characteristics of masonry through homogenization theory, *International Journal of Solids and Structures*, **32**(2), 137-163, 1995.

[21] P. Trovalusci, R. Masiani, Material symmetries of micropolar continua equivalent to lattices, *International Journal of Solids and Structures*, **36**(14), 2091-2108, 1999.

[22] A. Cecchi, K. Sab, A multi-parameter homogenization study for modeling elastic masonry, *European Journal of Mechanics A/Solids*, **21**, 249-268, 2002.

[23] F. Cluni, V. Gusella, Homogenization of non-periodic masonry structures, *International Journal of Solids and Structures*, **41**, 1911-1923, 2004.

[24] P. Trovalusci, A. Pau, Derivation of microstructured continua from lattice systems via principle of virtual works: the case of masonry-like materials as micropolar, second gradient and classical continua, *Acta Mechanica*, **225**(1), 157-177, 2014.

[25] Y.W. Kwon, D.H. Allen, R. Talreja, *Multiscale modeling and simulation of composite materials and structures*. Springer, 2008.

[26] F. Feyel, J.L. Chaboche, FE multiscale approach for modelling the elastoviscoplastic behaviour of long fibre SiC/Ti composite materials, *Computer Methods in Applied Mechanics and Engineering*, **183**(3), 309-330, 2000.

[27] S. Ghosh, K. Lee, P. Raghavan, A multi-level computational model for multi-scale damage analysis in composite and porous materials, *International Journal of Solids and Structures*, **38**(14), 2335-2385, 2001.

[28] F. Greco, L. Leonetti, P. Lonetti, A two-scale failure analysis of composite materials in presence of fiber/matrix crack initiation and propagation, *Composite Structures*, **95**, 582-597, 2013.

[29] F. Greco, L. Leonetti, P. Lonetti, P. Nevone Blasi, Crack propagation analysis in composite materials by using moving mesh and multiscale techniques, *Computers and Structures*, **153**, 201-216, 2015.

[30] R. Barretta, R. Luciano, J.R. Willis, On torsion of random composite beams, *Composite Structures*, **132**, 915-922, 2015.

[31] T. Sadowski, L. Marsavina, Multiscale modelling of two-phase Ceramic Matrix Composites, Computational Materials Science, 50, 1336-1346, 2011.

[32] L. Feo, F. Greco, L. Leonetti, R. Luciano, Mixed-mode fracture in lightweight aggregate concrete by using a moving mesh approach within a multiscale framework, *Composite Structures*, **123**, 88-97, 2015.

[33] F. Greco, L. Leonetti, R. Luciano, A multiscale model for the numerical simulation of the anchor bolt pull-out test in lightweight aggregate concrete, *Construction and Building Materials*, **95**, 860-874, 2015.

[34] R. Luciano, E. Sacco, Homogenization technique and damage model for masonry material, *International Journal of Solids and Structures*, **34**(24), 3191-3208, 1997.

[35] P. Trovalusci, R. Masiani, Non-linear micropolar and classical continua for anisotropic discontinuous materials, *International Journal of Solids and Structures*, **40**(5), 1281-1297, 2003.

[36] G. Milani, P.B. Lourenco, A. Tralli, Homogenised limit analysis of masonry walls, Part I: Failure surfaces, *Computers & Structures*, **84**(3-4), 166-180, 2006.

[37] T.J. Massart, R.H.J. Peerlings, M.G.D. Geers, An enhanced multi-scale approach for masonry wall computations with localization of damage, *International Journal for Numerical Methods in Engineering*, **69**, 1022-1059, 2007.

[38] S. Marfia, E. Sacco, Multiscale damage contact-friction model for periodic masonry walls, *Computer Methods in Applied Mechanics and Engineering*, **205-208**, 189-203, 2012.

[39] N. Cavalagli, F. Cluni, V. Gusella, Strength domain of non-periodic masonry by homogenization in generalized plane state, *European Journal of Mechanics, A/Solids*, **30**(2), 113-126, 2011.

[40] A. Caporale, F. Parisi D. Asprone, R. Luciano, A. Prota, Critical surfaces for adobe masonry: Micromechanical approach, *Composites Part B: Engineering*, **56**, 790-796, 2014.

[41] G. Milani, A. Taliercio, In-plane failure surfaces for masonry with joints of finite thickness estimated by a Method of Cells-type approach, *Computers and Structures*, **150**, 34-51, 2015.

[42] F. Greco, L. Leonetti, R. Luciano, P. Nevone Blasi, An adaptive multiscale strategy for the damage analysis of masonry modeled as a composite material, *Composite Structures*, **153**, 972-988, 2016.

[43] F. Greco, L. Leonetti, R. Luciano, P. Trovalusci, Multiscale failure analysis of periodic masonry structures with traditional and fiber-reinforced mortar joints, *Composites Part B: Engineering*, **118**, 75-95, 2017.

[44] S. Forest, K. Sab, Cosserat overall modeling of heterogeneous materials, *Mechanics Research Communications*, **25**(4), 449-454, 1998.

[45] F. Bouyge, I. Jasiuk, M. Ostoja-Starzewski, A micromechanically based couple-stress model of an elastic two-phase composite, *International Journal of Solids and Structures*, **38**, 1721-1735, 2001.

[46] R. Masiani, P. Trovalusci, Cosserat and Cauchy materials as continuum models of brick masonry, *Meccanica*, **31**(4), 421-432, 1996.

[47] A. Pau, P. Trovalusci, Block masonry as equivalent micropolar continua: the role of relative rotations, *Acta Mechanica*, **223**(7), 1455-1471, 2012.

[48] A. Lisjak, G. Grasselli, A review of discrete modeling techniques for fracturing processes in discontinuous rock masses, *Journal of Rock Mechanics and Geotechnical Engineering*, **6**(4), 301-314, 2014.

[49] P.B. Lourenco, J.G. Rots, Multisurface Interface Model for Analysis of Masonry Structures, *Journal of Engineering Mechanics*, **123**(7), 660-668, 1997.

[50] S. Forest, D.K. Trinh, Generalized continua and non-homogeneous boundary conditions in homogenisation methods, *ZAMM - Journal of Applied Mahematics and Mechanics*, **91**(2), 90-109, 2011.

[51] D. Addessi, M.L. De Bellis, E. Sacco, Micromechanical analysis of heterogeneous materials subjected to overall Cosserat strains, *Mechanics Research Communications,* 54, 27-34, 2013.

[52] X. Yuan, Y. Tomita, T. Andou, A micromechanical approach of nonlocal modeling for media with periodic microstructures, *Mechanics Research Communications*, **35**, 126-133, 2008.

[53] I.M. Gitman, H. Askes, L.J. Sluys, Coupled-volume multi-scale modelling of quasi-brittle material, *European Journal of Mechanics - A/Solids*, **27**(3), 302-327, 2008.

[54] COMSOL AB., *COMSOL Multiphysics reference manual*, 2017.

[55] N. Garg, C.S. Han, A penalty finite element approach for couple stress elasticity, *Computational Mechanics*, **52**(3), 709-720, 2013.

[56] O. Lloberas-Valls, D.J. Rixen, A. Simone, L.J. Sluys, On micro-to-macro connections in domain decomposition multiscale methods, *Computer Methods in Applied Mechanics and Engineering*, **225-228**, 177-196, 2012.

[57] T.M.J. Raijmakers, A.T. Vermeltfoort, *Deformation controlled tests in masonry shear walls - report B-92-1156*, Technical Report, Delft, The Netherlands: TNO-Bouw, 1992.

[58] P.B. Lourenco, *Computational strategies for masonry structures*, Doctoral Thesis, Delft University Press, 1996.

[59] P. Trovalusci, M.L. De Bellis, R. Masiani, A multiscale description of particle composites: From lattice microstructures to micropolar continua, *Composites Part B: Engineering*, **128**, 164-173, 2017.